SCATTERING PHASE MATRICES OF MODEL ENSEMBLES OF LARGE SPHERICAL PARTICLES

D.N. Romashov

Institute of Atmospheric Optics
Siberian Branch of the Russian Academy of Sciences, Tomsk
Received April 28, 1998

Some results of computer simulations of scattering phase matrices for visible radiation are presented for the case of large water spheres in air and for air bubbles in water. Two models of rain, that differ by the parameters of rain drop size-distribution function, are considered in this paper as well as two models of water suspension of air bubbles having different widths of the size spectra. Analysis of peculiarities in the angular behavior of the scattering phase matrix elements is being carried out for these two types of scattering media. Distinct manifestations of the rainbow effect of the first order and weak one of the second order rainbow are established for the air bubbles suspended in water, which are observed, on the contrary to water spheres in air, in the half-space of the forward scattering. Investigation of the effect of imaginary part of the refraction index on the scattering and backscattering efficiency is performed for water spheres at large values of the diffraction parameter (from 100 to 24000).

At present, vast material has been compiled on light scattering properties of hazes and clouds,[1–4] as well as on the extinction and transmission coefficients of precipitation,[5] in the form of both computer simulated and experimentally measured data. The work that is being presented in this paper has been aimed at filling in a gap in the numerical evaluation of the angular behavior of all elements of the scattering phase matrix in the visual region for ensembles of large particles that have nearly spherical shapes like the particles of liquid-drop precipitation and air bubbles in water.

Angular dependence of the scattering phase function and the degree of polarization of unpolarized light for the ensembles of large, almost spherical, particles with the real part of the refractive index more than 1 has been earlier investigated in Ref. 6. As for the case of particles with the refractive index below 1, no data have been found on the angular behavior of the scattering phase matrix elements.

1. SCATTERING BY WATER DROPLETS

One may find models of heavy, L, and weak, M, rain in Ref. 1. Calculations of all elements of the scattering phase matrix, as well as of the extinction and scattering coefficients were performed by the author for these two models and the radiation wavelength $\lambda = 0.69$ μm. The size distribution of droplets in the models is set by a modified gamma distribution with the following probability density function (m^{-3}·mm^{-1}):

$$n(r) = a \exp\left(-\frac{\alpha}{\gamma}\left(\frac{r}{r_{\mathrm{m}}}\right)^{\gamma}\right),\tag{1}$$

where r_{m} is the model radius; α, γ, and a are the parameters listed in Table I.

The values $r_{\max}$ and r_{eq} presented in this Table are the maximum and equivalent radii of a droplet; N and w are the mean values of droplet concentration and water content, respectively;

$$r_{\mathrm{eq}} = \int\limits_0^{\infty} n(r)\, r^3 \mathrm{d}r \Bigg/ \int\limits_0^{\infty} n(r)\, r^2 \mathrm{d}r .\tag{2}$$

The calculations according to Mie theory for large values of the diffraction parameter $x = 2\pi r/\lambda \approx 30000$ have been done using the RAIND program for drops and the BUBLED one for the bubbles that have been developed by the author based on the findings described Refs. 7 and 8. These programs were used to calculate light-scattering characteristics of large-droplet clouds[4] for $r \leq 150$ μm and $\lambda = 0.69$ μm, that is, for $x \leq 1366$.

TABLE I. Microphysical parameters for the rain models (see Ref. 1).

Rain model	N, m^{-3}	a	r_{m}, mm	$r_{\max}$, mm	r_{eq}, mm	α	γ	w, g/m^3
L	1000	$4.9757\cdot10^7$	0.07	2	0.47738	2	0.5	0.1167
M	100	$5.3333\cdot10^5$	0.05	3	0.86177	1	0.5	0.4948

The calculations made for the rain models L and M enabled numerical evaluations of the extinction, β_{ext}, and scattering, β_{sc}, coefficients. The calculated results are given in Table II.

TABLE II. Scattering and extinction coefficients for rains ($\lambda = 0.69$ μm; $n = 1.33 - i\,3.4 \cdot 10^{-8}$).

Rain model	β_{ext}, km^{-1}	β_{sc}, km^{-1}	ε_{ext}, km^{-1}
L	0.36462	0.36453	0.36669
M	0.81619	0.81582	0.86125

The value ε_{ext} listed in Table II is the extinction coefficient calculated using the approximate relation[9]

$$\varepsilon_{ext} = \frac{3}{2}\frac{w}{\rho\,r_{eq}}\,, \qquad (3)$$

where ρ is the density of water in g/m^3.

It is seen from Table II that equation (3) produces larger error in calculations for weak rains, which have a significant fraction of small particles, than for heavy rains.

Angular dependence of the four independent elements of the scattering phase matrix is shown in Fig. 1, where the solid line refers to a heavy rain, and the dashed line to a weak one. The element P_{11} of the scattering phase matrix satisfies the normalization condition

$$\int_0^\pi P_{11}(\theta)\,d\theta = 1\,. \qquad (4)$$

Here the normalization is performed by calculating the scattering coefficient in accordance with the exact Mie theory, while numerical determination of the integral (Eq. (4)) is performed using a grid of θ angles. The proximity of this integral to unity has been used as a criterion that the software procedure is correct.

It is seen from the behavior of curves shown in Fig. 1 that there are no significant differences between the angular dependence of all four elements described by the models used, except for the behavior of P_{11} in the angular range from 0 to 3° (Fig. 1a). One can see from Fig. 1 that the angular dependences of P_{11} element in the range from 3 to 180° coincide in both models. For illustration of the coincidence degree let us list the values P_{11} at three different angles from this range, where those are different to maximum degree: $P_{11}^L(4°) = 4.391$; $P_{11}^M(4°) = 4.258$; $P_{11}^L(138°) = 0.484$; $P_{11}^M(138°) = 0.438$; $P_{11}^L(180°) = 0.742$; $P_{11}^M(180°) = 0.7933$; here the superscripts denote the type of the rain model.
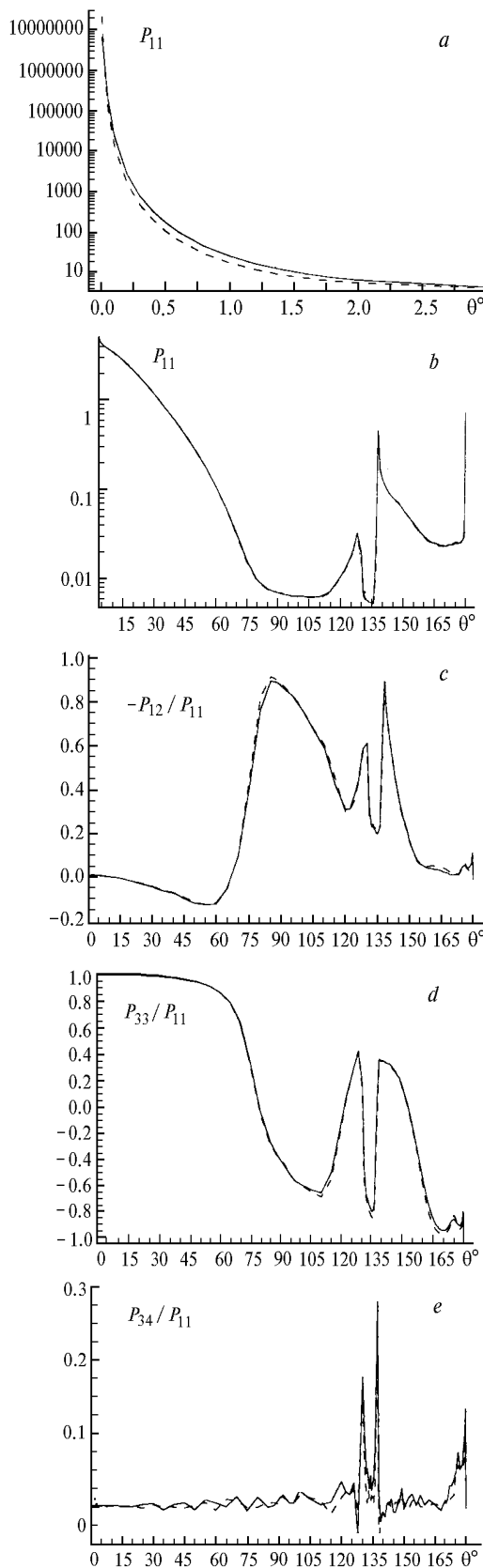

FIG. 1. Angular behavior of the scattering phase matrix elements for rain: model M (dashed curves), model L (solid curves).

Information on the imaginary part of the refractive index of the droplet substance is very important when modeling light scattering characteristics of large-droplet formations, as well as when interpreting sounding data on this formations obtained using visible radiation. It is confirmed by the calculated results, presented in Figs. 2 and 3.
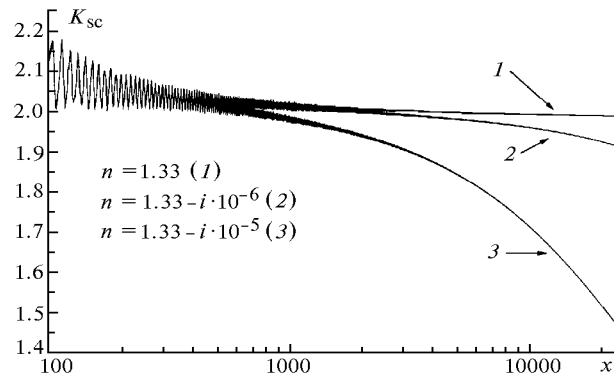

FIG. 2. Scattering efficiency factor K_{sc} as a function of the diffraction parameter x for spheres with equal real ($Re(n) = 1.33$) and different imaginary $m = Im(n)$ parts of the refractive index: $m = 0$ (1), $m = 10^{-6}$ (2), $m = 0^{-5}$ (3).

The dependences of the scattering efficiency factor K_{sc} on the diffraction parameter for the case of spheres with equal real while different imaginary parts of the refractive index are depicted in Fig. 2. Here the x axis is presented on the logarithmic scale ($x_{max} = 24000$). The behavior of the curves shows that the larger the imaginary part is, the faster is the asymptotic approach of K_{sc} to 1.

Behavior of the backscattering efficiency factor K_{π} is more sensitive to the value of the imaginary part of the refractive index, that is confirmed by the calculated results, depicted in Fig. 3. These results show that the oscillations of K_{π} are being smoothened more rapidly with the increasing imaginary part of the refractive index. In Ref. 1 one may found the relation for the limiting value of the backscattering efficiency, which is as follows:

$$\lim_{x \to \infty} K_{\pi}(n,x) = \left| \frac{n-1}{n+1} \right|^2. \qquad (5)$$

In the case when $Re(n) \gg Im(n)$, $\lim_{x \to \infty} K_{\pi}(1.33, x) \approx 0.02$. The calculations made for $n = 1.33 - i \cdot 10^{-5}$ (Fig. 3d) show that at $x > 24000$

$K_{\pi}(n, x) \le 0.04$, thus being close to its asymptotic limit.

2. LIGHT SCATTERING BY AIR BUBBLES SUSPENDED IN WATER

The question on microstructure of air bubbles suspended in water has been discussed in the literature too poorly that is obviously caused by its insufficient elaboration. So, two microphysical models, B1 and B2, of air bubbles in water presented in this paper are of purely heuristic nature thus being not meant to precisely describe realistic media. Basic parameters of the models constructed have been chosen based on experimental data.[10,11] Let us briefly consider the grounds for constructing the models. Sea waves, when falling down, trap some volume of air that finally results in creation of a large number of air bubbles in water. The bubbles can also appear due to the bombardment of the sea surface by the rain drops and the snow thaw as well. The experiments carried out by the authors of Ref. 12 (short analysis of which may be found in Ref. 10), showed that:

− the largest bubbles have diameter of 1500 μm;

− the smallest ones have diameter of 100 μm;

− the majority of bubbles have diameters below 200 μm;

− rain drops produce bubbles with the diameter about 50 μm;

− melting snow produces air bubble with the diameter of 40 μm.

In this connection, it was assumed that in the models B1 and B2 the bubble size-distribution function is described by a modified gamma-distribution with the probability density function set by Eq. (1). Distribution parameters α and γ were taken to be the same as in the cloud model C6,[4] because the drops in that type of clouds and bubbles in water have diameters smaller than 200 μm. Values of all the parameters accepted for models B1 and B2 are given in Table III.

The computer simulations were performed for radiation with wavelengths 0.355; 0.532; and 0.68 μm, which are most frequently used in sounding the ocean surface.[13] It is established that behavior of all four elements of the scattering phase matrix for both models, except only for the values P_{11} at small scattering angles, is the same at all wavelengths. Therefore, because of limited volume of a journal publication only model estimates of the scattering phase matrix for the radiation at 0.68 μm wavelength are presented in this paper (see Fig. 4).

TABLE III. Microphysical parameters for air bubble models.

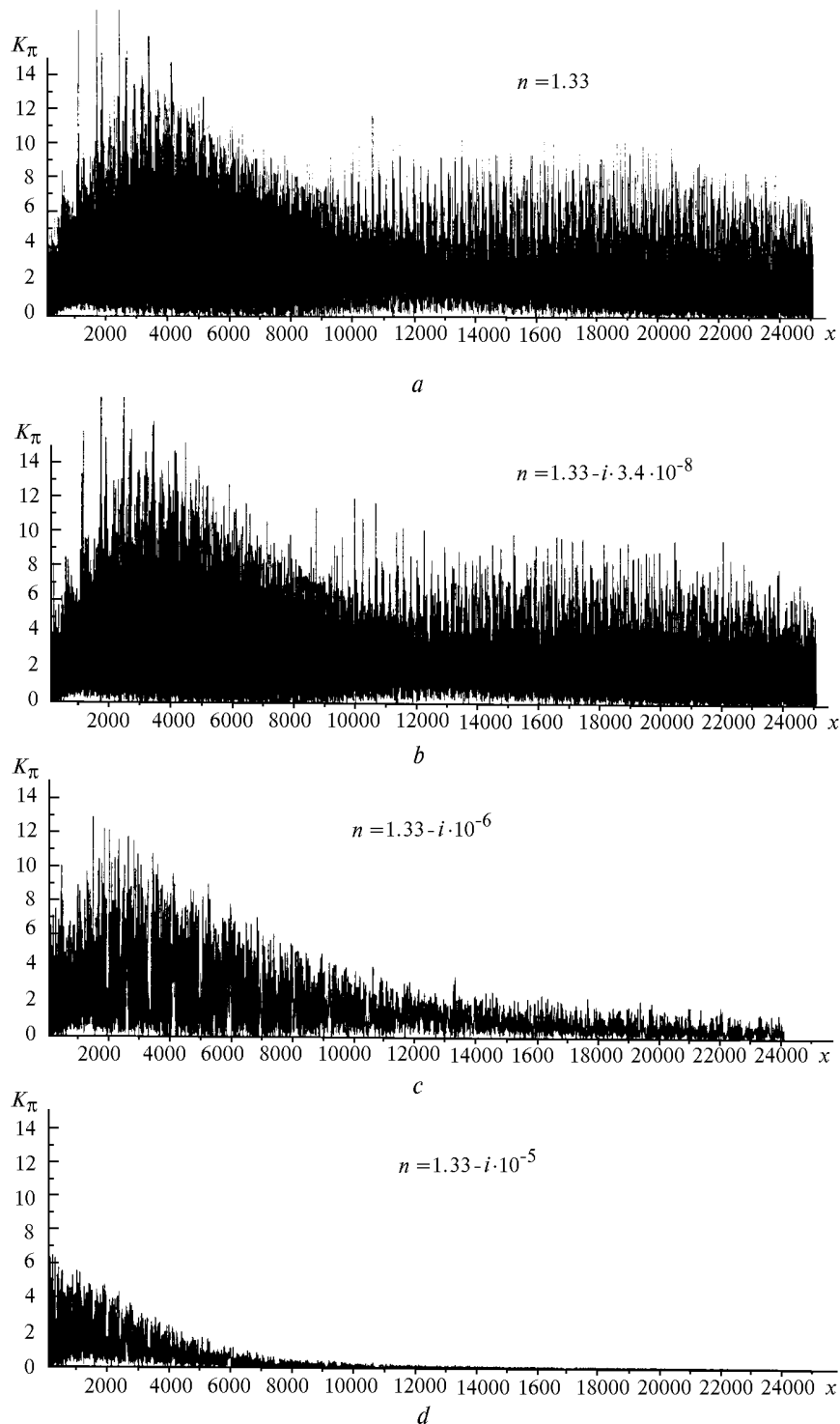| Model	N, cm^{-3}	a	r_m, μm	r_{max}, μm	r_{eq}, μm	α	γ	β_{ext}, km^{-1}
b 1	1	0.0005	20	750	50	2	1	5.2021
b 2	1	$6.25 \cdot 10^{-5}$	40	750	100	2	1	19.410

FIG. 3. *Backscattering efficiency factor K_π as a function of the diffraction parameter x for spheres with equal real* Re(n) = 1.33 *and different imaginary* m = Im(n) *parts of the refractive index n:* $m = 0$ *(a),* $m = 34 \cdot 10^{-9}$ *(b),* $m = 10^{-6}$ *(c),* $m = 10^{-5}$ *(d).*

It is a characteristic feature of light scattering by air bubbles in water that there is observed a clear manifestation of the rainbow of the first order near the scattering angle $\theta = 75°$ and with only weak rainbow of the second order near $\theta = 86°$ (Fig. 4*b*). The fact that no deep minimum occurs between the two rainbows in the case with air bubbles, that, on the contrary, is observed in light scattering by drops, can be explained by the contribution coming into the scattering field from diffraction, in this region of scattering angles. It is interesting to note that the element P_{34}/P_{11} has the values essentially different
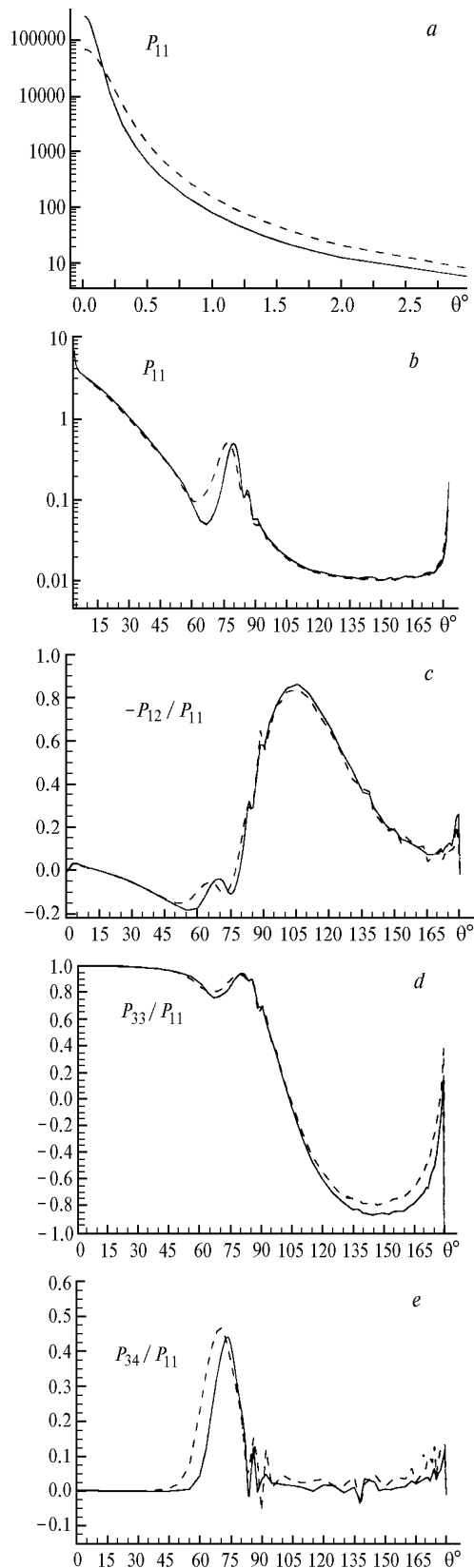
FIG. 4. The same as in Fig. 1 for air bubbles in sea water: model B1 (dashed curves), model B2 (solid curves).

than zero in a wide range of scattering angles $50° < \theta < 80°$ (Fig. 4e). That may be explained by the effect of total internal reflection when radiation reaches the water-air interface for the first time. The last column of Table III contains the values of the extinction coefficient (in this case it is equal to the scattering coefficient) for each model of air bubbles suspended in water, as calculated using Mie theory. The extinction of radiation in water with air bubbles occurs due to scattering on bubbles and absorption of light by water. Behaviors of the extinction efficiency factor K_{ext} of air bubbles in water and water drops in air are shown in Fig. 5 (curve 1 and curve 2, respectively) as functions of the diffraction parameter x. The refractive index n of water is taken to be equal to 1.33. It is noticeable from the behavior of the efficiency factor K_{ext} that the approximation, that assumes $K_{ext} \approx 2$, for ensembles of large air bubbles in water, as is normally accepted for water drops in air, results in smaller errors of the extinction coefficient evaluation by Eq. (3). The absence of ripple on the extinction curve for an air sphere in water is explained by the absence of induced multipole fields inside it, since it is just these resonances that give rise to ripple structure in the case of $Re(n) > 1$, where n is the relative refractive index of the sphere.
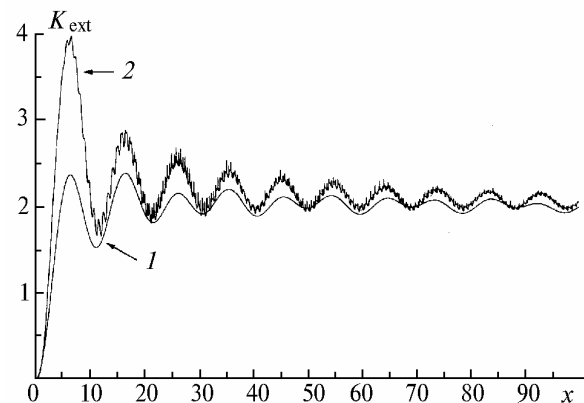

FIG. 5. The extinction efficiency factor K_{ext} as a function of the diffraction parameter x for the air spheres in water (1), for the water sphere in air (2).

The calculated results presented here and their analysis could be useful for specialists in radiation transfer through the atmosphere and ocean, since it enables taking into account certain corrections for the factors discussed in the paper.

REFERENCES

1. D. Deirmendjian, *Electromagnetic Scattering on Spherical Polydispersions* (American Elsevier, New York, 1969).
2. G.M. Krekov and R.F. Rakhimov, *Optical Sounding Model of Continental Aerosol* (Nauka, Novosibirsk, 1982) 198 pp.

3. V.E. Zuev and G.M. Krekov, *Optical Models of the Atmosphere* (Gidrometeoizdat, Leningrad, 1986), 256 pp.

4. O.E. Bazhenov, E.I. Kasiyanov, and D.N. Romashov, Atmos. Oceanic Opt. **5**, No. 3, 150–154 (1992).

5. E.A. Polyakova, Trudy Gl. Geofiz. Obs., issue 100, 52–59 (1960).

6. J.K. Peltoniemi, K.K. Lumme, K. Muinonen, and M.V. Irvin, Appl. Opt. **28**, No. 19, 4088–4095 (1989).

7. J. Seltman, Geophys. u. Veroff. d. KMU. Leipzig. Bd. III., H. 2, Berlin, 171–185 (1985).

8. A.A. Akulinin, Opt. Atm. **1**, No. 6, 127–129 (1988).

9. K.Ya. Kondratiev and V.I. Binenko, *Cloud Effect on Radiation and Climate* (Gidrometeoizdat, Leningrad, 1984), 240 pp.

10. Ya.E. Geguzin, *Bubbles* (Nauka, Moscow, 1985), 173 pp.

11. A.H. Perri and J.H. Worker, *The Ocean-Atmosphere System* (Gidrometeoizdat, Leningrad, 1979), 195 pp.

12. D.C. Blanchard and A.N. Woodcock, Tellus, A Quarterly Journal of Geophysics **9**, No. 2, 146–158 (1957).

13. *Oceanic Optics. Applied Oceanic Optics* (Nauka, Moscow, 1983), Vol. 2, 237 pp.